DOI: 10.1002/ejic.200700407

Inclusion Complexes for Use in Room-Temperature Gas-Sensor Design

Liwei Mi,[a] Hongwei Hou,*[a] Jiaqiang Xu,[b] Hong Xu,[a] Zhiyong Song,[a] Mingsheng Tang,[a] and Yaoting Fan[a]

Keywords: Inclusion compounds / Semiconductors / Sensors / Density functional calculations / Bridging ligands

The inclusion complex $[\{Co(bpy)(H_2O)_4\}\cdot(fcds)]_n$ (**1**), which has been constructed using the guest molecule ferrocene-1,1′-disulfonate (fcds), the bridging ligand 4,4′-bipyridine (bpy) and d^7 Co^{2+}, contains an infinite zigzag chain formed by the central Co^{II} ion and the bridging bpy ligand. Guest fcds molecules lie between two adjacent zigzag chains. The highly conjugated structure of complex **1** means that it can be used as a metal-organic semiconductor, and it also shows a high response to liquefied petroleum gas (LPG) and ethanol/petroleum ether (EP) at room temperature. The inclusion complexes $[\{Co(bpp)_2(H_2O)_2\}\cdot(fcds)\cdot 4H_2O]_n$ [**2**; bpp = 1,3-bis(4-pyridyl)propane] and $[\{Zn(bpy)(H_2O)_4\}\cdot(fcds)]_n$ (**3**), on the other hand, cannot be employed as room-temperature gas sensors because they are insulators. The electrical resistivity of inclusion complex $[\{Ni(bpy)(H_2O)_4\}\cdot(fcds)]_n$ (**4**) is 621 MΩ, whereas that of $[\{Co(bpy)(H_2O)_4\}SO_4\cdot(4\text{-abaH})_2\cdot 3H_2O]_n$ (**5**) (4-abaH = 4-aminobenzoic acid) is only 137 MΩ. This means that the semi-conducting properties of such inclusion complexes depend on both the conjugated structure and the central metal ions. Furthermore, conjugated inclusion complexes with an odd number of electrons could be useful for the design of highly selective room-temperature gas sensors.

Introduction

Research into low-cost, selective, sensitive and reliable room-temperature gas-sensitive materials has become increasingly important because gas management has become an issue of vital significance in these environmentally conscious times.[1] For this reason, many inorganic oxide semiconductors, such as SnO_2, TiO_2 and WO_2, have been used as gas sensors.[2] However, their lack of long-term stability and selectivity has prevented the widespread use of this type of sensor. Current research into state-of-the-art gas sensors is focused on metallophthalocyanine (MPC)-based semiconductors due to their high response to many gases at room temperature.[3] Undoped conventional MPCs are insulators and their semi-conducting properties are derived from their most noticeable feature, namely their highly charged conjugated electron system, the readily accessible π and π* orbitals of which allow at least partial oxidization or reduction of the macrocycle with gases such as NO_2 or O_3.[4]

Our strategy for creating room-temperature gas sensors utilizes metal-organic inclusion complexes[5] because they have already been proved to be promising materials for gas storage and molecular recognition[6] and they can easily be prepared under moderate conditions. Furthermore, metal-organic complexes usually contain highly conjugated metal organic hosts with highly charged conjugated electron systems and ionic guest molecules. We believe that both the highly conjugated systems and the central metals govern the gas-sensitive properties of inclusion complexes, which is in contrast to MPC-based gas sensors, where the π-conjugated system contributes mostly to their semiconducting properties.[7] To verify this assumption, four inclusion complexes[8] containing the guest molecule ferrocene-1,1′-disulfonate (fcds), namely $[\{Co(bpy)(H_2O)_4\}\cdot(fcds)]_n$ (**1**), $[\{Co(bpp)_2(H_2O)_2\}\cdot(fcds)\cdot 4H_2O]_n$ (**2**), $[\{Zn(bpy)(H_2O)_4\}\cdot(fcds)]_n$ (**3**), $[\{Ni(bpy)(H_2O)_4\}\cdot(fcds)]_n$ [**4**; bpy = 4,4′-bipyridine, bpp = 1,3-bis(4-pyridyl)propane], and the inclusion complex[9] $[\{Co(bpy)(H_2O)_4\}SO_4\cdot(4\text{-abaH})_2\cdot 3H_2O]_n$ (**5**; 4-abaH = 4-aminobenzonic acid), which contains the neutral molecule 4-abaH as guest, were synthesized. Complexes **1**, **4**, and **5** show some semi-conducting behavior under an adscititious voltage of 5.0 V. However, only **1** exhibits a high response to gasoline and liquefied petroleum gas at room temperature as both **2** and **3** are insulators under these conditions. Quantum chemical calculations help to reveal some of the mechanisms involved in room-temperature gas-sensor design from inclusion complexes (Scheme 1).

[a] Department of Chemistry, Zhengzhou University, Henan 450052, China
Fax: +86-371-6776-1744
E-mail: houhongw@zzu.edu.cn
[b] College of Materials and Chemical Engineering, Zhengzhou University of Light Industry, Henan 450002, China

Supporting information for this article is available on the WWW under http://www.eurjic.org or from the author.

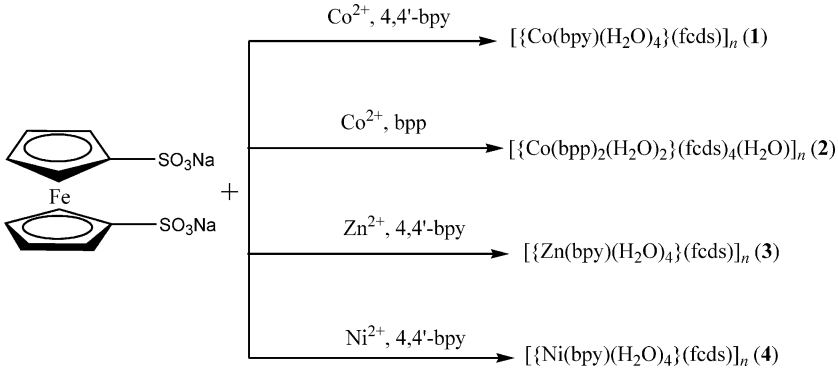

Scheme 1.

Results and Discussion

Complex **1** was prepared by combining odd-electron divalent Co^{2+} ions with highly conjugated 4,4′-bpy ligands and disodium ferrocene-1,1′-disulfonate. The molecular structure of **1** consists of two parts. The cationic component $[Co(bpy)(H_2O)_4]^{2+}$ forms an infinite zigzag chain, and fcds makes up the anionic part of **1**. As shown in Figure 1, the central cobalt ions lie at the center of a distorted octahedron formed by four oxygen atoms from water molecules

Table 1. Selected bond lengths [Å] and angles [°] for **1**–**3**.[a]

		1	
Co(1)–O(4)#1	2.0851(19)	Co(1)–O(4)	2.0851(19)
Co(1)–O(5)#1	2.126(2)	Co(1)–O(5)	2.126(2)
Co(1)–N(1)	2.1511(19)	Co(1)–N(1)#1	2.1511(19)
O(4)#1–Co(1)–O(4)	91.89(12)	O(4)#1–Co(1)–O(5)#1	90.63(8)
O(4)–Co(1)–O(5)#1	85.82(8)	O(4)#1–Co(1)–O(5)	85.82(8)
O(4)–Co(1)–O(5)	90.64(8)	O(5)#1–Co(1)–O(5)	174.90(10)
O(4)#1–Co(1)–N(1)	176.88(8)	O(4)–Co(1)–N(1)	90.84(8)
O(5)#1–Co(1)–N(1)	91.06(8)	O(5)–Co(1)–N(1)	92.66(8)
O(4)#1–Co(1)–N(1)#1	90.84(8)	O(4)–Co(1)–N(1)#1	176.88(8)
O(5)#1–Co(1)–N(1)#1	92.66(8)	O(5)–Co(1)–N(1)#1	91.06(8)
N(1)–Co(1)–N(1)#1	86.47(11)		
		2	
Co(1)–O(4)	2.072(4)	Co(1)–O(4)#1	2.072(4)
Co(1)–N(1)#1	2.205(4)	Co(1)–N(1)	2.205(4)
Co(1)–N(2)#2	2.218(4)	Co(1)–N(2)#3	2.218(4)
O(4)–Co(1)–O(4)#1	180.0(2)	O(4)–Co(1)–N(1)#1	91.83(15)
O(4)#1–Co(1)–N(1)#1	88.17(15)	O(4)–Co(1)–N(1)	88.17(15)
O(4)#1–Co(1)–N(1)	91.83(15)	N(1)#1–Co(1)–N(1)	180.000(2)
O(4)–Co(1)–N(2)#2	89.26(15)	O(4)#1–Co(1)–N(2)#2	90.74(15)
N(1)#1–Co(1)–N(2)#2	93.68(15)	N(1)–Co(1)–N(2)#2	86.32(15)
O(4)–Co(1)–N(2)#3	90.74(15)	O(4)#1–Co(1)–N(2)#3	89.26(15)
N(1)#1–Co(1)–N(2)#3	86.32(15)	N(1)–Co(1)–N(2)#3	93.68(15)
N(2)#2–Co(1)–N(2)#3	180.000(1)		
		3	
Zn(1)–O(4)	2.084(2)	Zn(1)–O(4)#2	2.084(2)
Zn(1)–O(5)#2	2.138(3)	Zn(1)–O(5)	2.138(3)
Zn(1)–N(1)#2	2.162(3)	Zn(1)–N(1)	2.162(3)
O(4)–Zn(1)–O(4)#2	91.07(14)	O(4)–Zn(1)–O(5)#2	85.99(11)
O(4)#2–Zn(1)–O(5)#2	85.99(11)	O(4)#2–Zn(1)–O(5)	85.99(11)
O(4)–Zn(1)–O(5)	90.61(11)	O(4)–Zn(1)–N(1)#2	176.87(11)
O(5)#2–Zn(1)–O(5)	175.16(14)	O(5)#2–Zn(1)–N(1)#2	92.27(11)
O(4)#2–Zn(1)–N(1)#2	91.55(10)	O(4)–Zn(1)–N(1)	91.55(10)
O(5)–Zn(1)–N(1)#2	91.27(10)	O(5)#2–Zn(1)–N(1)	91.27(10)
O(4)#2–Zn(1)–N(1)	176.87(11)	N(1)#2–Zn(1)–N(1)	85.88(15)
O(5)–Zn(1)–N(1)	92.27(11)		

[a] Symmetry transformations used to generate equivalent atoms: **1**: #1 $-x - 1, y, -z - 1/2$; **2**: #1 $-x + 3, -y + 2, -z + 3$; #2 $-x + 3, -y + 2, -z + 2$; #3 $x, y, z + 1$; **3**, #1 $-x + 1/2, -y + 3/2, -z$; #2 $-x, y, -z - 1/2$; #3 $-x, -y, -z$.

and two nitrogen atoms from two 4,4′-bpy ligands. The coordinated water molecules form strong hydrogen bonds with the anionic part, with the shortest bond being only 1.854 Å and the longest one 3.013 Å. These bonds make the structure very stable (Tables 1 and 2).

Figure 2 shows that the cationic metal-organic and the anionic organic chains are arrange alternately along the *c* axis. The $[Co(bpy)_2(H_2O)_4]^{2+}$ chains are parallel with a distance of 8.478 Å, which gives rise to a highly conjugated structure, as proved by subsequent quantum calculations. These calculations were conducted at the density functional theory (DFT) level using the LanL2DZ basis set.[10] The results of these calculations show that the frontier molecular orbitals of **1** are primarily based on conjugated fcds [HOMO(α): 49.42%; LUMO(α): 48.75%] and the aryl groups of the bpy pillars [HOMO(α): 50.08%; LUMO(α): 50.81%], as depicted in Figure 3. This means that the whole structure of **1** is highly conjugated and that delocalization of the π-electron cloud might make the electron transfer easier. We can therefore deduce that inclusion complexes can be synthesized with semiconducting properties by a judicious choice of highly conjugated organic layers and guest molecules. The charge-transport properties of conjugated polymers in some organic semiconductors,[11] for example, are very closely associated with their π-electron clouds.[12]

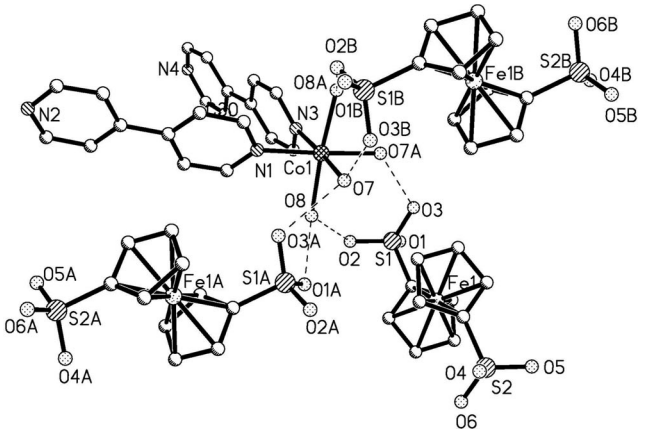

Figure 1. Building block of $[\{Co(bpy)(H_2O)_4\}\cdot(fcds)]_n$ (**1**). Hydrogen atoms have been omitted for clarity. The dotted lines represent hydrogen bonds.

Table 2. Important hydrogen bonds in **1**–**3**.[a]

D–H	A	*d*(D–H)	*d*(D···H)	*d*(D···A)	D–H–A [°]
		1			
O(4)–H(4F)	O(3)#1	0.65(3)	2.14(3)	2.790(3)	178(4)
O(4)–H(4F)	S(1)#1	0.65(3)	3.01(3)	3.611(2)	155(3)
O(5)–H(5E)	O(1)#2	0.77(3)	2.02(3)	2.783(3)	179(3)
O(5)–H(5F)	O(2)	0.80(3)	1.95(3)	2.756(3)	174(3)
O(4)–H(4E)	O(3)	0.90(4)	1.85(4)	2.723(3)	166(3)
O(4)–H(4E)	S(1)	0.90(4)	2.92(4)	3.760(3)	156(3)
		2			
O(4)–H(4F)	O(3)#1	0.88(6)	1.84(7)	2.703(5)	170(6)
O(4)–H(4F)	S(1)#1	0.88(6)	3.07(7)	3.901(4)	160(5)
O(4)–H(4E)	O(2)#2	0.89(2)	1.86(3)	2.731(5)	164(6)
O(5)–H(5E)	O(1)#3	0.85(6)	1.97(6)	2.816(7)	171(6)
O(5)–H(5E)	S(1)#4	0.85(6)	2.94(6)	3.701(5)	149(5)
O(6)–H(6E)	O(1)#4	0.86(2)	2.21(13)	2.942(9)	143(19)
O(5)–H(5F)	O(3)	0.86(8)	2.17(8)	3.016(7)	168(7)
O(5)–H(5F)	O(2)	0.86(8)	2.64(8)	3.255(8)	129(6)
O(5)–H(5F)	S(1)	0.86(8)	2.91(8)	3.722(6)	158(6)
O(6)–H(6E)	O(5)	0.96(9)	1.84(9)	2.799(8)	173(8)
		3			
O(4)–H(4E)	O(2)#1	0.75(5)	2.06(5)	2.788(3)	166(6)
O(4)–H(4E)	S(1)#1	0.75(5)	2.90(5)	3.611(3)	161(5)
O(5)–H(5E)	O(1)#2	0.66(3)	2.14(3)	2.789(4)	173(4)
O(4)–H(4F)	O(2)	0.76(4)	2.00(4)	2.731(4)	162(4)
O(4)–H(4F)	S(1)	0.76(4)	3.04(4)	3.771(3)	163(4)
O(5)–H(5F)	O(3)	0.85(5)	1.90(5)	2.743(4)	171(4)

[a] Symmetry transformations used to generate equivalent atoms: **1**: #1 $-x-1, -y, -z$; #2 $x, -y, z-1/2$; **2**: #1 $x+1, y, z+1$; #2 $-x+2, -y+1, -z+2$; #3 $-x+1, -y+1, -z+1$; #4 $x+1, y, z$; **3**: #1 $-x, -y+1, -z$; #2 $x, -y+1, z-1/2$.

It should be noted that various gases can be detected by measuring the change of electrical conductivity induced on a suitable active layer by the absorption of gas molecules on its surface.[1a] This change in the conducting behavior of gas-sensing materials results in their use in gas sensors, although to obtain excellent gas sensors the materials must first of all be semiconductors.

The guest fcds molecules in the solid-state structure are found in the space between two adjacent $[Co(bpy)(H_2O)_4]^{2+}$-containing metal-organic layers (interlayer distance: 8.992 Å). This gives rise to numerous O–H···O hydrogen bonds, the shortest of which are only 1.854 Å. It has been reported that the sorption strength of organic compounds

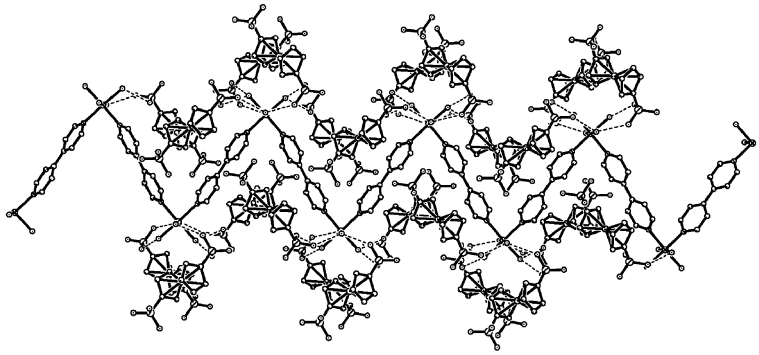

Figure 2. X-ray structure of the pillared and layered structures in solid **1**. Hydrogen atoms have been omitted for clarity.

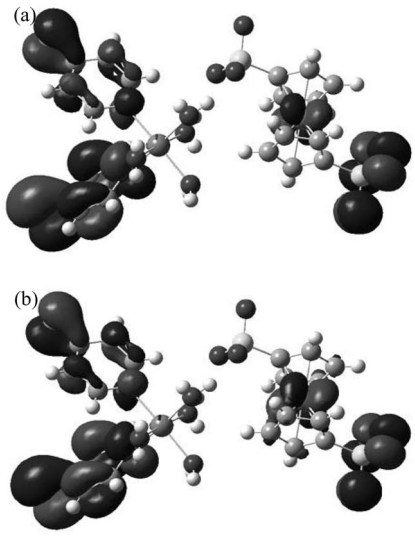

Figure 3. The frontier molecular orbitals of **1**: a) HOMO(α); b) LUMO(α).

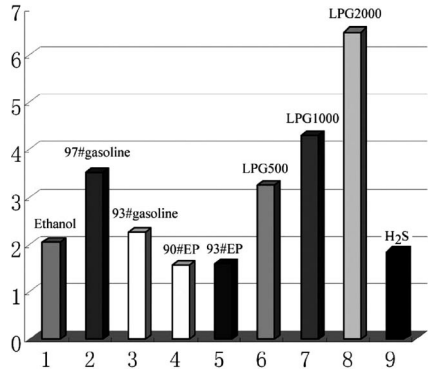

Figure 4. Selectivity of **1** to different gases at room temperature.

depends on similar weak interactions (H-bridge bonds, dispersion forces),[13] therefore the weak interactions in inclusion complexes, especially the H-bonds and π-π interactions between the aryl groups of the pyridine pillars and fcds guests, also contribute to the gas-sensing properties of these complexes. Thus, **1** should have an excellent gas response.

We measured the response of **1** to H_2S (concentration: 50 ppm), ethanol (50 ppm), liquefied petroleum gas (LPG; 50, 1000, and 2000 ppm), 97# gasoline (50 ppm), 93# gasoline (50 ppm), 90# ethanol/petroleum ether (EP; 50 ppm), and 93# ethanol/petroleum ether (EP; 50 ppm) using a commercial gas-sensing measurement system containing HW-30 with no conductive binder added [90# and 97# denote the motor octane number (MON) of the gasoline]. The gas-sensitivity curve was obtained by measuring the change of conductivity at room temperature. As shown in Figure 4, complex **1** displays much higher responses to LPG, EP, gasoline, and alcohol. This behavior is different to that of metal-substituted PCs, which only show a response to highly reactive gases such as NO_2, NH_3, Cl_2, CO, and N_2.[14] For comparison, we also measured the selectivity of **1** to gases such as NO_2, N_2, CO, and NH_3; no response was obtained.

The experiment results show that polymeric cobalt inclusion complex **1** could be useful for identifying gases such as LPG, EP, gasoline, alcohol, and H_2S due to its special crystal structure, which contains plenty of hydrogen bonds. However, complex **1** shows no response to NO_2, N_2, CO, and NH_3. The following possibilities must be considered regarding the difference between NO_2, N_2, CO, NH_3, and H_2S. The first is that N_2, CO, and NO_2 cannot easily coordinate to the central cobalt ion in complex **1** because this ion is coordinatively saturated by four coordinated water molecules and two nitrogen atoms from two adjacent 4,4′-bipy bridging ligands. Accordingly, complex **1** cannot be used to identify N_2, CO, and NO_2. Secondly, both H_2S and NH_3 can easily form hydrogen bonds with complex **1**. Previous literature reports have shown that the room-temperature sensing of H_2S gas is possible due to a heterocontact-type sensing mechanism,[15,16] and we believe that a similar mechanism might be functioning in our inclusion complexes. However, the sensing mechanism for NH_3 gas is very different to that of H_2S, so it is easy to understand why complex **1** can identify H_2S and not NH_3.

There are many holes in the crystal structure of **1** which can accommodate numerous small organic gas molecules. The high response of the cobalt inclusion compound to LPG, EP, gasoline, and alcohol at room temperature might be caused by its highly conjugated structure, which possesses a large number of hydrogen bonds, although the regular arrangement of the anionic fcds-containing parts may also enhance the selectivity of this compound. Compound **1** could be reused after heating the gas sensor for a short time, although it should be noted that the selectivity of **1** is slightly lower in the reversible absorption process. This mechanism of action of an inclusion complex contrasts with that of metal-substituted PCs as the latter always contain an unsaturated central metal ion, while the divalent iron ions in our synthesized complex also lie at the center of two negative univalent cyclopentadienyl ions. MPCs could, however, serve as reactive gas sensors. Metal oxide sensor materials also respond to small gas molecules, although most of them only work at high temperature.[17]

A combined TGA-DSC analysis was carried out to study the thermal behavior of inclusion complex **1**. The experiments were performed with samples containing numerous single crystals of each compound under N_2/air at a heating rate of 10 °C min^{-1}. Crystals of **1** undergo two major weight losses at around 140 and 320 °C (Figure 5). The first weight loss between 140 and 180 °C corresponds to the removal of four coordinated water molecules (calcd. 11.40%; found 11.28%). The remaining compound remained nearly intact until 320 °C, beyond which it decomposed. This thermal behavior study shows that this complex should remain intact after heating to release testing gases such as LPG, EP, gasoline and alcohol.

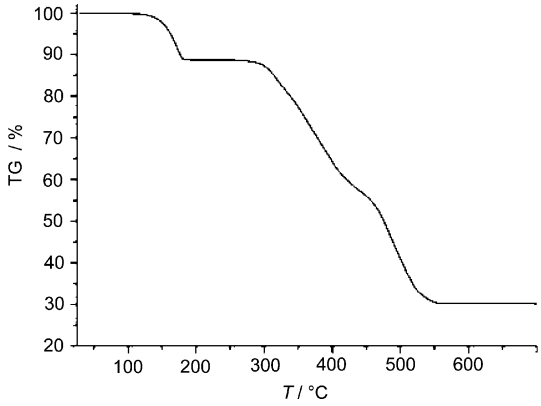

Figure 5. TGA curve of inclusion complex **1**.

Complex **2**, which contains the less conjugated ligand bpp instead of 4,4′-bpy, was synthesized under the same conditions as **1** to check that the gas-sensing properties of inclusion complexes originate from their conjugated π-electron clouds. This complex contains a different motif with double-stranded chains of loops, although it also contains the cationic component $[Co(bpp)_2(H_2O)_2]^{2+}$ and the anionic part contains fcds. As shown in Figure 6, each cobalt center is coordinated by four nitrogen atoms from four bridging bpp ligands and two oxygen atoms from two solvent water molecules. Two nitrogen atoms are nearly coplanar and two oxygen atoms occupy the axial positions. The Co–N bond lengths are 2.205, 2.205, 2.218, and 2.218 Å and all the Co–O bonds are equivalent (2.072 Å). This gives rise to a slightly distorted octahedron. The packing structure of **2** (Figure 7) shows that the double-stranded chain of loops is constructed from central Co^{II} cations and bpp bridging ligands. Due to the long Co···Co distance (11.716 Å) and the distance between the middle carbon atoms of the two diametrically opposing $CH_2CH_2CH_2$ spacers (9.206 Å), the fcds guest molecules do not further bridge Co^{II} cations. It should be noted that these structural factors, especially the introduction of the less conjugated ligand bpp, greatly reduce the conjugation of the whole structure, as was also confirmed by theoretical calculations. The frontier molecular orbitals of **2** (Figure 8) mainly arise from the contribution of the anionic part [HOMO(α): 99.98%; LUMO(α): 99.86%], while the aryl groups of the bpp pillars in **2** contribute very little to these orbitals [HOMO(α): 0.0024%; LUMO(α): 0.14%]. It is therefore clear that only part of **2** is highly conjugated, which means that **2** should show no gas-sensing properties. Indeed, **2** exhibits no response to gases since it shows high electronic resistivity in measurements performed under the same conditions as for **1**.

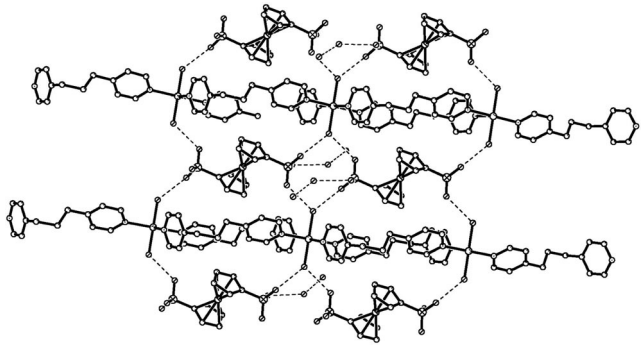

Figure 7. The 3D packing structure of **2**. Hydrogen atoms have been omitted for clarity.

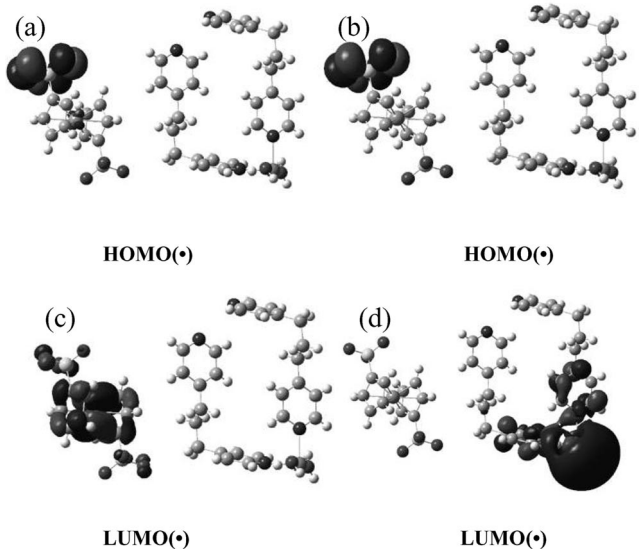

Figure 8. The frontier molecular orbitals of $[\{Co(bpp)_2(H_2O)_2\}\cdot(fcds)\cdot 4H_2O]_n$: a) HOMO(α); b) HOMO(β); c) LUMO(α); d) LUMO(β).

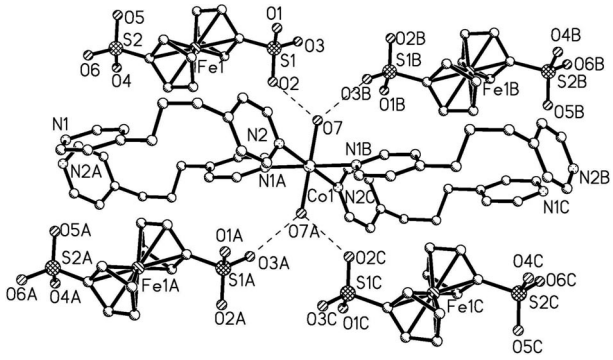

Figure 6. The molecular unit of $[\{Co(bpp)_2(H_2O)_2\}\cdot(fcds)\cdot 4H_2O]_n$ (**2**). Hydrogen atoms have been omitted for clarity.

It has been proven both experimentally and theoretically that highly conjugated molecules can be used as electron conductors.[18] The semiconducting properties of metal-organic inclusion complexes should, however, also depend on the appropriate selection of metal ions. This was further tested by the synthesis of **3**.

The molecular structure of **3** should be highly conjugated as it contains the d^{10} Zn^{2+} cation instead of Co^{2+}, highly conjugated 4,4′-bpy and fcds. This complex was synthesized under the same conditions as for **1**. The structure of **3** and its packing are shown in Figures 9 and 10, respectively. Compound **3** has essentially the same molecular structure

as **1** but with slightly different bond lengths and angles. The calculations also show that the aryl groups of the 4,4′-bpy pillars and the anionic parts in **3**, respectively, contribute to the frontier molecular orbitals (HOMO: 27.00 and 72.93%; LUMO: 72.66 and 27.16%). Similar to **1**, the whole crystal structure of **3** is highly conjugated. However, in contrast to **1**, **3** displays no gas-sensing properties because the experimental data show that it is an insulator. This means that a highly conjugated structure is not the governing factor in room-temperature metal-organic gas-sensor design. Obviously, the choice of central metal ion also affects the conductivity of metal-organic inclusion complexes. This was confirmed by considering the electronic structures of the central metal ions. The Co 3d orbitals in Co complexes are split due to the odd number of electrons. Cobalt is a typical divalent transition metal and Co complexes have the ability to function as electron-transfer intermediates by permitting a high electron-transfer probability.[19] However, divalent zinc complexes do not permit one-electron reduction due to their spin-coupled electronic structures and the tertiary ionization energy of zinc ions is significantly higher than that of cobalt ions, therefore **3** does not show gas-sensing properties due to its high electrical resistance.

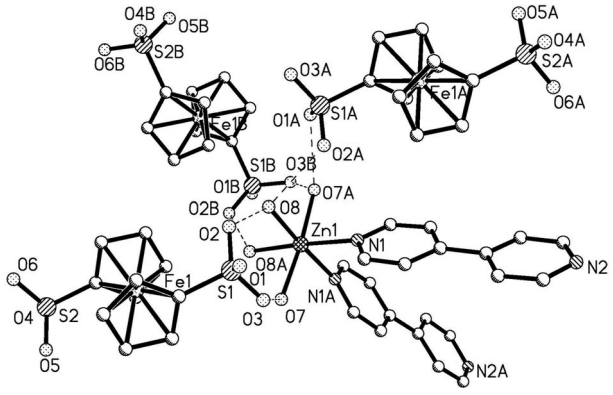

Figure 9. Coordination structure of $[\{Zn(bpy)(H_2O)_4\}\cdot(fcds)]_n$ (**3**). Hydrogen atoms have been omitted for clarity.

Complex **4**, which contains d^8 Ni^{2+} instead of Co^{2+} or Zn^{2+}, was prepared according to the synthetic method for **1** or **3**. Complexes **1**, **3**, and **4** show extremely similar IR spectra and complexes **1** and **3** have the same molecular structure, which led us to expect that complex **4** would also have the same structure. Elemental analyses and UV/Vis spectra for powdered samples of **1** and **4** were also recorded. The solid UV reflectance spectra of **1** and **4** are shown in Figure 11. It is clear that these compounds have similar solid-state UV spectra, therefore it is likely that **1** and **4** have the same structures expect for the central metal ions.

The gas-sensitivity test showed that the electric resistivity of **4** is 621 MΩ, lower than that of **3** but much higher than that of **1** (1.86 MΩ) as this nickel complex is likely to be low-spin.[20] A comparison of **1** with **3** and **4** showed that besides the highly conjugated systems, the central metal atoms are of significant importance for obtaining a perfect inclusion complex based gas sensor. This was further validated by the gas-sensitivity test of complex $[\{Co(bpy)(H_2O)_4\}SO_4\cdot(4\text{-abaH})_2\cdot 3H_2O]_n$ (**5**). Similar to the structure of **1**, the molecular structure of **5** is also made up of two parts, namely the cation $[Co(bpy)(H_2O)_4]^{2+}$, which forms an infinite chain with neutral 4-abaH, and the SO_4^{2-} anion and lattice water. The electrical resistivity of **5** is 137 MΩ, which is lower than that of **4**, because the central metal atom in **5** is d^7 cobalt. Clearly, inclusion complexes with an odd number of electrons are more suitable for use as gas sensors. The electrical resistivity of **5** is higher than that of **1**, and **5** shows only a small response to H_2S and liquefied petroleum gas as its anionic moiety is different to that in **1**.

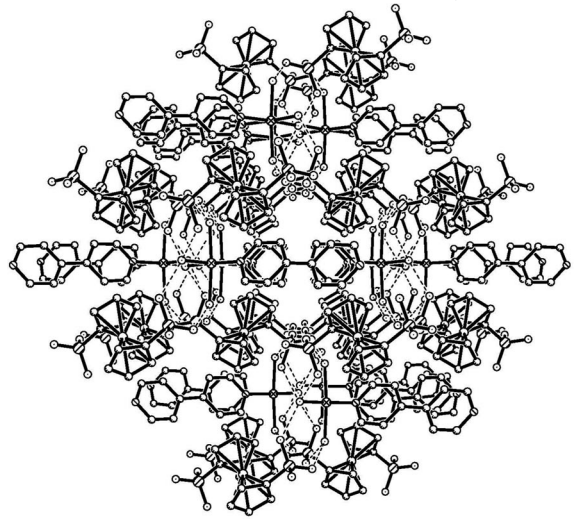

Figure 10. Crystal packing structure of **3**. Hydrogen atoms have been omitted for clarity.

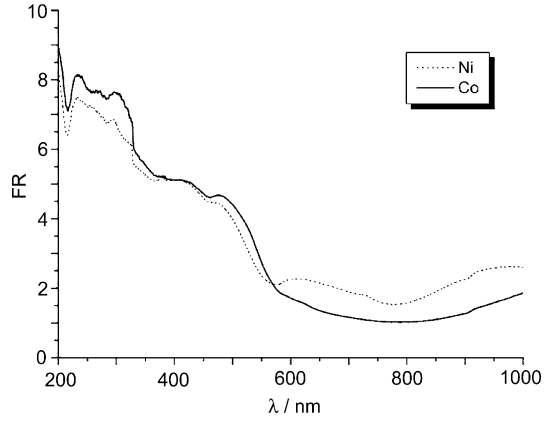

Figure 11.The solid UV reflectance spectra of **1** and **4**.

Conclusions

The semiconducting cobalt inclusion compound **1** shows a high response to LPG, EG, and gasoline. Inclusion compounds **2** and **3** can not, however, be used as gas sensor because they are insulators. Complexes **4** and **5** have also been synthesized. A comparison of these five complexes has shown that both highly conjugated systems and the appro-

priate central metal ions are important factors in the design of room-temperature gas sensors containing metal-organic inclusion complexes. This study may be useful in the search for new gas-sensitive materials.

Experimental Section

1: This complex was prepared by treating $CoCl_2 \cdot 6H_2O$ (0.0238 g, 0.1 mmol) with one equivalent of Na_2fcds (0.0390 g, 0.1 mmol) and two equivalents of 4,4′-bipy (0.0312 g, 0.2 mmol) in a mixture of methanol (4 mL) and water (2 mL). The desired complex crystallized at room temperature as a red crystalline solid upon slow evaporation of the solvents. Yield 0.056 g (89%). $C_{20}H_{24}CoFeN_2O_{10}S_2$: calcd. C 38.05, H 3.83, N 4.44, S 10.16; found C 38.21, H 3.88, N 4.38, S 10.13. IR (KBr): $\tilde{\nu}$ = 3300 (s), 1612 (s), 1532 (s), 1418 (m), 1200 (s), 1042 (s), 1013 (m), 823 (m), 731 (m), 637 (s), 481 (s) cm^{-1}.

2: A methanol solution (3 mL) of Na_2fcds (0.0390 g, 0.1 mmol) was added to a methanol solution (2 mL) of $CoCl_2 \cdot 6H_2O$ (0.0238 g, 0.1 mmol). After stirring for a while, the mixture was added to an ethanol solution of bpp (0.0396 g, 0.2 mmol) then allowed to stand in air at room temperature for a week. This procedure gave red crystals suitable for X-ray diffraction. Yield 0.037 g (41%). $C_{36}H_{48}CoFeN_4O_{12}S_2$ (907.70): calcd. C 47.64, H 5.33, N 6.17, S 7.07; found C 47.61, H 5.38, N 6.28, S 6.93. IR (KBr): $\tilde{\nu}$ = 3439 (s), 3243 (s), 2947 (m), 1615 (s), 1426 (s), 1182 (s), 1041 (s), 839 (m), 642 (s), 493 (s) cm^{-1}.

3: Complex **3** was prepared in a similar manner to **1** but with $ZnCl_2$ instead of $CoCl_2 \cdot 6H_2O$. Yield 0.052 g (81%). $C_{20}H_{24}FeN_2O_{10}S_2Zn$ (637.76): calcd. C 38.05, H 3.83, N 4.44, S 10.06; found C 37.96, H 3.86, N 4.49, S 10.09. IR (KBr): $\tilde{\nu}$ = 3453 (s), 1612 (s), 1418 (m), 1120 (s), 1067 (s), 810 (m), 659 (s), 499 (s) cm^{-1}.

4: Complex **4** was also prepared in a similar manner to **1** but with $NiCl_2 \cdot 6H_2O$ instead of $CoCl_2 \cdot 6H_2O$. Yield 0.052 g (83%). $C_{20}H_{24}FeN_2NiO_{10}S_2$ (631.09): calcd. C 38.06, H 3.83, N 4.44, S 10.16; found C 38.18, H 3.91, N 4.51, S 9.98. IR (KBr): $\tilde{\nu}$ = 3339 (s), 1612 (s), 1418 (m), 1199 (s), 1041 (s), 823 (m), 639 (s), 481 (s) cm^{-1}.

Crystallographic Studies: Diffraction intensity data for the single crystal of **1** were collected at room temperature with a Bruker Smart CCD diffractometer equipped with graphite-monochromated Mo-K_α radiation (λ = 0.71073 Å). The structures were solved by direct methods and refined by full-matrix least-squares techniques on F^2 with anisotropic thermal parameters for all non-hydrogen atoms.[21] Hydrogen atoms were located geometrically and refined isotropically.

Gas-Sensitivity Test: Gas sensors were made from as-prepared single crystals of inclusion complexes **1**–**5**. The single crystals were moistured with ethanol and ground in an agate mortar to form a powdery paste. This paste was coated on an alumina tube on which a pair of Au electrodes had previously been printed and dried at room temperature in air. The gas sensitivity was measured in the static state. The tested gases (C_2H_5OH, HCHO, NH_3, and LPG, 90# gasoline, CO, O_2 and N_2) were injected into a test bottle and mixed with air. The measuring electrical circuit for the gas sensors is shown in the electronic supporting information. The resistivity of the sensor in air or a test gas can be measured by monitoring V_{out}. The gas sensitivity (response magnitude) in this paper was defined as $S = R_a/R_g$, where R_a and R_g are the resistivity of a sensor in air and in the test gas, respectively.

Supporting Information (see also the footnote on the first page of this article): Crystallographic data for **1**–**3**. Figure S1 shows the selectivity of **1** to different gases at room temperature, Figure S2 displays the selectivity of **1** to CO and NH_3 at room temperature. Figure S3 displays the frontier molecular orbital of $\{[Zn(bpy)(H_2O)_4](fcds)\}_n$, Figure S4 the IR spectra of **1**, **3** and **4**.

Acknowledgments

This work was supported by the National Natural Science Foundation of China (grant nos. 20371042 and 20671082) and NCET.

[1] a) R. Rella, A. Serra, P. Siciliano, A. Tepore, L. Valli, A. Zocco, *Langmuir* **1997**, *13*, 6562–6567; b) J. Spadavecchia, G. Ciccarella, R. Rella, *Sens. Actuators, B* **2005**, *106*, 212–220; c) N. Pinna, G. Neri, M. Antonietti, M. Niederberger, *Angew. Chem. Int. Ed.* **2004**, *43*, 4345–4349; d) Z. L. Wang, *Adv. Mater.* **2003**, *15*, 432–436.

[2] a) N. S. Lewis, *Acc. Chem. Res.* **2004**, *37*, 663–672; b) J. W. Grate, *Chem. Rev.* **2000**, *100*, 2627–2648; c) R. W. J. Scott, S. M. Yang, N. Coombs, G. A. Ozin, D. E. Williams, *Adv. Funct. Mater.* **2003**, *13*, 225–231; d) W. Y. Li, L. N. Xu, J. Chen, *Adv. Funct. Mater.* **2005**, *15*, 851–857; e) N. Shirahata, W. Shin, N. Murayama, A. Hozumi, Y. Yokogawa, T. Kameyama, Y. Masuda, K. Koumoto, *Adv. Funct. Mater.* **2004**, *14*, 580–588; f) J. Polleux, A. Gurlo, N. Barsan, U. Weimar, M. Antonietti, M. Niederberger, *Angew. Chem. Int. Ed.* **2006**, *45*, 261–265; g) J. Q. Xu, Y. P. Chen, D. Y. Chen, J. N. Shen, *Sens. Actuators B* **2006**, *113*, 526–531.

[3] a) S. Chakane, A. Gokarna, S. V. Bhoraskar, *Sens. Actuators, B* **2003**, *92*, 1–5; b) B. Wang, X. Zuo, Y. Q. Wu, Z. M. Chen, Z. Li, *Mater. Lett.* **2005**, *59*, 3073–3077; c) R. D. Yang, B. Fruhberger, J. Park, A. C. Kummel, *Appl. Phys. Lett.* **2006**, *88*, 074104/1–074104/3.

[4] G. Guillaud, J. Simon, J. P. Germain, *Coord. Chem. Rev.* **1998**, *178–180*, 1433–1484.

[5] a) L. Fabbrizzi, F. Foti, S. Patroni, P. Pallavicini, A. Taglietti, *Angew. Chem. Int. Ed.* **2004**, *43*, 5073–5077; b) K. A. Kellersberger, J. D. Anderson, S. M. Ward, K. E. Krakowiak, D. V. Dearden, *J. Am. Chem. Soc.* **2001**, *123*, 11316–11317; c) W. Y. Sun, T. Kusukawa, M. Fujita, *J. Am. Chem. Soc.* **2002**, *124*, 11570–11571; d) T. Uemura, R. Kitaura, Y. Ohta, M. Nagaoka, S. Kitagawa, *Angew. Chem. Int. Ed.* **2006**, *45*, 4112–4114; e) H. Kim, H. Chun, G. H. Kim, H. S. Lee, K. Kim, *Chem. Commun.* **2006**, 2759–2761.

[6] a) S. A. Dalrymple, G. K. H. Shimizu, *Chem. Commun.* **2006**, 956–958; b) Y. F. Zhou, F. L. Jiang, D. Q. Yuan, B. L. Wu, R. H. Wang, Z. Z. Lin, M. C. Hong, *Angew. Chem. Int. Ed.* **2004**, *43*, 5665–5668; c) H. J. Choi, M. P. Suh, *J. Am. Chem. Soc.* **2004**, *126*, 15844–15851.

[7] a) R. M. Rosa, R. L. Szulc, R. W. C. Li, J. Gruber, *Macromol. Symp.* **2005**, *229*, 138–142; b) R. Schlaf, B. A. Parkinson, P. A. Lee, K. W. Nebesny, N. R. Armstrong, *J. Phys. Chem. B* **1999**, *103*, 2984–2992.

[8] **1**: $C_{20}H_{24}CoFeN_2O_{10}S_2$, M = 631.31, monoclinic, space group $C2/c$, a = 17.893(4), b = 12.163(2), c = 13.371(3) Å, β = 84.7360(11)°, V = 2483.09(6) Å^3, Z = 4, D_c = 1.689 Mgm^{-3}, R = 0.0280 and Rw = 0.0644; **2**: $C_{36}H_{48}CoFeN_4O_{12}S_2$, M = 907.68, triclinic, space group $P\bar{1}$, a = 9.5100(19), b = 9.977(2), c = 11.716(2) Å, α = 96.33(3)°, β = 107.86(3)°, γ = 102.96(3)°, V = 1011.7(3) Å^3, Z = 1, D_c = 1.490 Mgm^{-3}, R = 0.0601 and Rw = 0.1545; **3**: $C_{20}H_{24}FeN_2O_{10}S_2Zn$, M = 637.75, monoclinic, space group $C2/c$, a = 17.855(4), b = 12.213(2), c = 13.351(3) Å, β = 121.27(3)°, V = 2488.4(9) Å^3, Z = 4, D_c = 1.702 Mgm^{-3}. R = 0.0363 and Rw = 0.0848. CCDC-612722 (for **1**), -612723 (for **2**) and -612724 (for **3**) contain the supplementary crystallographic data for this paper. These data can be obtained free of

charge from The Cambridge Crystallographic Data Centre via www.ccdc.cam.ac.uk/data_request/cif.
[9] H. J. Chen, *Chin. J. Struct. Chem.* **2005**, *24*, 236–240.
[10] a) M. J. Frisch, G. W. Trucks, H. B. Schlegel, G. E. Scuseria, M. A. Robb, J. R. Cheesman, J. A. Motgomery Jr., T. Vreven, K. N. Kudin, J. C. Burant, J. M. Millam, S. S. Iengar, J. Tomasi, V. Barone, B. Mennucci, M. Cossi, G. Scalmani, N. Rega, G. A. Petersson, H. Nakatsuji, M. Hada, M. Ehara, K. Toyota, R. Fukuda, J. Hasegawa, M. Ishida, T. Nakajima, Y. Honda, O. Kitao, H. Nakai, M. Klene, X. Li, J. E. Knox, H. P. Hratchian, J. B. Cross, C. Adamo, J. Jaramillo, R. Gomperts, R. E. Stratmann, O. Yazyev, A. J. Austin, R. Cammi, C. Pomelli, J. W. Ochterski, P. Y. Ayala, K. Morokuma, G. A. Voth, P. Salvador, J. J. Dannenberg, V. G. Zakrzewski, S. Dapprich, A. D. Daniels, M. C. Strain, O. Farkas, D. K. Malick, A. D. Rabuck, K. Raghavachari, J. B. Foresman, J. V. Ortiz, Q. Cui, A. G. Baboul, S. Clifford, J. Cioslowski, B. B. Stefanov, G. Liu, A. Liashenko, P. Piskorz, I. Komaromi, R. L. Martin, D. J. Fox, T. Keith, M. A. al-Laham, C. Y. Peng, A. Nanayakkara, M. Challacombe, P. M. W. Gill, B. Johnson, W. Chen, M. W. Wong, C. Gonzalez, J. A. Pople, *Gaussian 03*, Revision B.03, Gaussian, Inc., Pittsburgh, PA, **2003**; b) H. W. Hou, Y. L. Wei, Y. L. Song, L. W. Mi, M. S. Tang, L. K. Li, Y. T. Fan, *Angew. Chem. Int. Ed.* **2005**, *44*, 6067–6074; c) C. Risko, G. P. Kushto, Z. H. Kafati, J. L. Bredas, *J. Chem. Phys.* **2004**, *121*, 9031–9038.
[11] J. S. Huang, M. Kertesz, *J. Phys. Chem. B* **2005**, *109*, 12891–12898.
[12] a) A. Facchetti, M. H. Yoon, C. L. Stern, H. E. Katz, T. J. Marks, *Angew. Chem. Int. Ed.* **2003**, *42*, 3900–3903; b) C. J. Tonzola, M. M. Alam, W. Kaminsky, S. A. Jenekhe, *J. Am. Chem. Soc.* **2003**, *125*, 13548–13558; c) G. R. Hutchison, M. A. Ratner, T. J. Marks, *J. Am. Chem. Soc.* **2005**, *127*, 16866–16881.
[13] K. Bodenhöfer, A. Hierlemann, J. Seemann, G. Gauglitz, B. Koppenhoefer, W. Göpel, *Nature* **1997**, *387*, 577–582.
[14] F. Geobaldo, B. Onida, P. Rivolo, S. Borini, L. Boarino, A. Rossi, G. Amato, E. Garrone, *Chem. Commun.* **2001**, 2196–2197.
[15] L. A. Patil, D. R. Patil, *Sens. Actuators, B* **2006**, *120*, 316–323.
[16] G. H. Jain, L. A. Patil, *Sens. Actuators, B* **2007**, *123*, 246–253.
[17] J.-M. Barbe, G. Canard, S. Brandès, F. Jérôme, G. Dubois, R. Guilard, *Dalton Trans.* **2004**, 1208–1214.
[18] J. M. Seminario, A. G. Zacarias, J. M. Tour, *J. Am. Chem. Soc.* **2000**, *122*, 3015.
[19] a) S. Brooker, P. G. Plieger, B. Moubaraki, K. S. Murray, *Angew. Chem. Int. Ed.* **1999**, *38*, 408–410; b) L. M. Yan, J. M. Seminario, *J. Chem. Phys. A* **2005**, *109*, 6628–6633.
[20] a) I. M. Angulo, E. Bouwman, S. M. Lok, M. Lutz, W. P. Mul, A. L. Spek, *Eur. J. Inorg. Chem.* **2001**, *6*, 1465–1473; b) K. Kurzak, A. Gonciarz, I. Kuzniarska-Biernacka, *Pol. J. Chem.* **2005**, *79*, 47–56.
[21] a) G. M. Sheldrick, *SHELXS 97, Program for the Solution of Crystal Structures*, University of Göttingen, Germany, **1997**; b) G. M. Sheldrick, *SHELXL 97, Program for the Refinement of Crystal Structures*, University of Göttingen, Germany, **1997**.

Received: April 13, 2007
Published Online: October 2, 2007

